Composite nanofibres of CuI-polystyrene via electrospinning through critical control of solvation conditions

Received: 22 May 2024 | Revised: 26 August 2024 | Accepted: 9 September 2024

DOI: 10.1002/app.56322

RESEARCH ARTICLE

Applied Polymer SCIENCE WILEY

Composite nanofibres of CuI-polystyrene via electrospinning through critical control of solvation conditions

Muaathe A. Ibraheem[1] | **Fred J. Davis**[2] | **Saeed D. Mohan**[3] | **John E. McKendrick**[2]

[1]Department of Chemistry, College of Sciences, University of Diyala, Ba'aqubah, Diyala, Iraq

[2]School of Chemistry, Food, and Pharmacy, University of Reading, Whiteknights, Reading, Berkshire, UK

[3]Chemical Analysis Facility, JJ Thomson Laboratory, University of Reading, Whiteknights, Reading, Berkshire, UK

Correspondence
Muaathe A. Ibraheem, Department of Chemistry, College of Sciences, University of Diyala, Ba'aqubah, Diyala, Iraq.
Email: m.a.ibraheem@pgr.reading.ac.uk; muaathe.a@gmail.com

Saeed D. Mohan, Chemical Analysis Facility, JJ Thomson Laboratory, University of Reading, Whiteknights, Reading, Berkshire RG6 6ED, UK.
Email: s.mohan@reading.ac.uk

Funding information
Iraqi Ministry of Higher Education and Scientific Research

Abstract

Composite nanofibres of copper (II) with various polymer matrices have been frequently reported. However, due to the lack of solubility of the Cu(I) moieties, Cu(I) electrospinning has proved more challenging. The objective of this study was to find a route to and prepare nanofibres containing copper iodide. This investigation describes the successful electrospinning of composite nanofibres of copper iodide (CuI) and polystyrene (PS) using a combination of two solvents to provide critical spinning conditions. The electrospinning solution was prepared by combining dimethylformamide (DMF) as the main solvent for PS and triethylamine (TEA) as a cosolvent; this mediates the dissolution of CuI. Electrospinning was accomplished under different parameters such as PS concentration, CuI concentration, and applied voltage. The outcome of the process was colored and smooth nanofibres that underwent analysis using scanning electron microscopy (SEM), energy dispersive X-ray (EDX), X-ray diffraction (XRD) and inductively coupled plasma - mass spectrometry (ICP-MS). The analysis findings emphasized the importance of the electrospinning parameters, specifically the concentration of PS and the applied voltage on successful fiber generation. However with control of these conditions composite nanofibres of CuI-PS with uniform distribution of nanoscale crystallites of CuI can be successfully produced.

KEYWORDS

composites, copper (I) iodide, electrospinning, fibers

1 | INTRODUCTION

In many disciplines, nanotechnology has a long history of addressing challenging and sophisticated issues.[1,2] As a class of nanomaterial, nanofibres have a number of unique physical and chemical properties, making them ideal for a wide range of commercial and research applications. With cross-sectional diameters ranging from tens nanometer up to the submicron scale, these materials possess a high specific surface area and area-to-volume

ratio; as a result, they can form highly porous mesh networks with excellent connectivity between their pores,[3] which is a highly desirable feature for advanced applications.[4,5]

Nanofibres can be produced by several approaches including phase separation, template synthesis, electrospinning, and so forth.[5] Nevertheless, electrospinning has been mooted as being the most cost-effective and highly versatile method of producing nanofibres. As a part of the Electrospinning process, various natural and synthetic polymers are spun electrostatically to form nanofibrous mats. In this technique, an ejected polymer or melt solution is driven by a high electrostatic potential and collected as dried nanofibres on a grounded collector. Moreover, it can incorporate various essential materials (organic or inorganic species), which is no surprise given its adaptability as a suitable technique for different technological demands.[2]

Although hundreds of publications annually explore nanofibre production, applications for typical nanofibres made from conventional polymers are still limited.[5] To increase the range of potential applications, composite nanofibres of two or more incorporated materials are increasingly being explored.[6] It is well-known that blending suitable species into hosting polymers results in a combination of features of the blended materials. By carefully selecting the additive species, it is possible to integrate varied properties to meet specific requirements of electrical, optical, and even bioactive characteristics in a flexible matrix. This straightforward technique is the principal subject matter of numerous publications in composite nanofibres production, creating applications ranging from membranes,[7] protective coatings,[8] catalysis,[9] and drug-delivery[10]; Composite nanofibres with mineral species like Nickel,[11] Cobalt,[12] and Copper[13] have been frequently reported with the aim of incorporating minerals within the electrospun fibers. In this regard, a range of options exist for the introduction of the mineral component. Thus one approach relies on the ready availability of many nanoparticles which can be included as a suspension in the polymer electrospinning solution; for example Liang et al., while developing battery technology, have electrospun gelatin fibers containing zeolitic imidazolate framework-67 and C_{60} directly from a suspension of these materials in the polymer solution.[14] Similarly polyurethane/carbon nanotube composites have been prepared from a suspension of these in solvent, although the authors quote difficulties with phase separation.[15] In this laboratory we found the use of a surfactant helpful in the preparation of carbon nano tube polymer composites.[16] However, others have found prior ultrasonication to be sufficient to disperse nanoparticles, as in the elegant experiments of Chen et al.[17] who developed porous photocatalytic nanofibres based on titanium dioxide and poly(ethersulphone). In contrast, Aravind et al. have prepared inorganic nanofibres of Ag—TiO_2 through hydrothermal synthesis.[18] In many cases inorganic materials have been incorporated into nanofibres simply through dissolving an inorganic salt and a polymer in a suitable solvent (often for subsequent manipulation of the inorganic material—see below); while precipitating/crystallizing out into the fiber gives less control than the direct addition of well-defined, nanoparticles, it does offer a simplified approach which is particularly suitable if scale up is required.

In general, it has been reported that mineral composite nanofibres can undergo conversion to their corresponding oxides through the process of heat treatment and calcination. This transformation has been observed in several studies and provides a promising avenue for the development of new materials with improved properties.[19] Ideally, choosing the right mineral source is the starting point for achievable and smooth electrospinning practice; in this way the mineral species needs to be soluble in the electrospun solution. In the case of copper composites, nanofibres were explored relatively early, starting from the work of Bognitzki et al. as they produced PVB-$Cu(NO_3)_2$ composite nanofibres which were then pyrolyzed and reduced to produce metallic copper fibers[20]; by the same approach Wang et al produced PAN-$Cu(OAc)_2$ nanofibres which was followed with calcination,[13] and this has since become a guideline procedure to prepare CuO nanofibres for subsequent metalation, just with the minor revision of adopting different spinning polymers or Cu(II) soluble moieties.[21,22]

There is considerable interest in applications of nanofibres and particularly nanofibres produced by electrospinning.[23] Composite materials offer further opportunities; as a consequence of the scale of the fibers, incorporated particles might be expected to show some of the many useful, unusual and often tunable properties of nanoparticles[24] which may impart, for example desirable optical,[25,26] thermal,[27] and magnetic[28] behaviors. Copper (II) composite nanofibres are among the earliest nanofibres to be successfully developed into a commercial product.[23] However, despite over 15 years of exploration into copper composite nanofibres,[13,22] there have been few reported successful attempts related to Cu(I) composite nanofibres, particularly those related to Cu(I) halides. This is due to the fact that they are sparingly soluble in water or common organic solvents. However, copper iodide (CuI) is a material of substantial promise; its unique properties and characteristics have made cuprous iodine a topic of great interest to researchers. A particularly noticeable feature of CuI is that it has an electronic structure which makes it

appealing for use in electronic and optoelectronic devices. This includes not only a large band gap but also negative spin-orbit splitting, which has a remarkable association with the quantum well and optoelectronics.[29,30] Other favorable features include its large temperature dependency, anomalous diamagnetism behavior, and ionicity and have led to widespread applications in fields, including nonlinear optics, solar cell manufacturing,[31] photocatalysis,[32] photoluminescence,[33] and in superionic conductors.[34] CuI is also well-known as a catalyst for the synthesis of organic compounds in a variety of processes.[35]

In view of the studies described above we have concluded there is a clear need to create CuI-polymer nanofibres. For example, such fibers could be exploited as active materials for filtration. Copper iodide nanoparticles have been found to inactivate SARS-CoV-2[36] and have also been found to be active against both gram-negative and gram-positive bacteria[37]; furthermore filtration efficiency increases with a decrease in fiber diameter.[38] In addition, these materials offer potential as solid supported catalysts with a major simplification of the process of catalyst removal post reaction; for example copper iodide nanoparticles have been shown to be effective catalysts for the synthesis of alkynyl esters.[39] In this contribution we describe the successful production of fine and uniform CuI-PS nanofibres through careful experimentation using a critical solvation technique with a combination of two solvents. Furthermore, these studies reveal the importance of thorough postproduction analysis when dealing with such systems.

2 | MATERIALS AND METHODS

All materials were used without any further purification, polystyrene (PS) (avg. MW of 350,000), Dimethylformamide (DMF), CuI (99.5%) and Triethylamine (99%) (TEA) were obtained from Sigma Aldrich. The electrospinning process was performed at the University of Reading using a local design setup, a high-voltage power supply from Glassman of positive polarization type capable of delivering 0–30 kV and a syringe pump from Razel Scientific. The spun fibers were examined by X-ray diffractometer (XRD; D8 Advance, Bruker) with Cu Kα ($\lambda = 1.5418$ Å). A sample of electrospun fibers for electron microscope analysis were coated with Gold and examined using a Cambridge Instruments Stereoscan 360 and TESCAN Mira SEMs. The average diameter of at least 100 spun fibers was measured utilizing ImageJ software. Quantitative measurement of copper concentrations in a bulk collection of fibers was performed using a ThermoFisher Scientific iCAP Q Inductively Coupled Plasma Mass Spectrometer (ICP-MS). Samples with a typical mass of 1–2 mg were digested with nitric acid/ hydrogen peroxide prior to introduction to the mass spectrometer and concentrations were determined with reference to suitable standard solutions.

TABLE 1 Electrospinning solutions prepared for electrospinning studies.

Solution code	DMF (mL)	TEA (mL)	PS % w/v	CuI % w/v
MY121	8	2	16	1
MY122	8	2	16	3
MY123	8	2	16	5
MY124	8	2	12.8	3
MY125	8	2	10.4	3

All PS solutions were dissolved in DMF without any use of heating or stirring. The dissolution process took 7 days to fully dissolve the PS in DMF before any further material was added. After that, a fixed amount of TEA was added, and then CuI was added to the solution and left to dissolve for another 4 days. Three concentrations of PS were prepared (16, 12.8, and 10.4 w/v %) with 3% w/v CuI; the solution with a higher percentage of PS was also prepared with different amounts of CuI (1%, 3%, 5% w/v); the solutions used in these investigations are listed in Table 1.

Nanofibres were produced using the electrospinning process at fixed and long collection distances of 20 cm. Similarly, the flow rate of the electrospinning solution was also set at a relatively high flow rate of 7.62 mL/h. A series of experiments were conducted using polymer solutions with moderate to low concentrations. Furthermore, three different positive polarization high voltages were applied as the main parameter to evaluate their impact on the spinning products. All runs utilized medium-sized blunt needles of 17 gauge, and the electrospun fibers were collected on aluminium foil on a grounded drum collector. The electrospinning process was only performed under low humidity conditions (typically 23 ± 3 RH%) and at an ambient temperature of around 22°C. A comprehensive list of the electrospinning process parameters can be found in Table 2.

3 | RESULTS AND DISCUSSION

Optimum conditions for smooth electrospinning required careful selection of solvents and preparation of solutions. Suitable solvents for both PS and CuI are limited but the inorganic material is soluble in TEA and PS in DMF. The PS remained in solution with the addition of 20% of

TEA (a mixture of TEA and dioxalane was also used but results in terms of smooth fiber formation were found to be more variable). The ratio of the two solvents was critical for these experiments, since even with a slightly lower amount of TEA the copper iodide started to precipitate. Thus, more rapid evaporation of TEA during spinning prompted early solidification of the inorganic component; evaporation of small amounts of DMF had little effect on the PS solution. The second factor critical for smooth electrospinning was the dissolution of the polymer over several days (7 days were typically used) without the use of stirring. Solutions used in the absence of this procedure were less reliable in terms of smooth fiber formation. The precise origin of this observation is not clear at present, but we note stirring of high molecular weight polymers has been associated with the formation of aggregates,[40] and in the case of aqueous whey protein solutions with the breaking up of aggregates; in this later case facilitating electrospinning.[41]

TABLE 2 Electrospinning process parameters of spinning PS-CuI composites.

Exp code	Solution code	Voltage KV	RH%	Temp. C
MET149	MY121	17.5	25.4	17.4
MET150	MY121	20	25.9	19.6
MET151	MY121	22.5	22.6–23.8	20–19
MET152	MY122	17.5	25.8	22.6–23
MET153	MY122	20	22	20–19.8
MET154	MY122	22.5	19–22	22–19
MET155	MY123	17.5	22	22.7–23
MET156	MY123	20	21	23–22.7
MET157	MY123	22.5	22.6	24.8
MET158	MY124	17.5	26	21.8
MET159	MY124	20	23–26	21.8–21.3
MET160	MY124	22.5	23–25	21.8–21.4
MET161	MY125	17.5	21.7	24.6
MET162	MY125	20	19.6	24.5
MET163	MY125	22.5	19.6	24.3

Driven by an electrostatic high voltage positive potential, continuous spinning of beige nanofibres was achieved in excellent yields. These fibers were subjected to thorough examination and analysis using SEM–EDX and XRD. The primary observation of the produced fine fibers supports the project's aim of creating nanofibres containing CuI, as evidenced by the relatively thick mats of off-white fibers (presumably due to iodine produced by decomposition)[42] shown in Figure 1.

The concept of this process is built on synchronized solvents evaporation; from this perspective, the TEA solvent plays a crucial role as a base and in the regard that it helps to dissolve the Cu(I) moiety. With a substantially lower boiling point, this co-solvent has a higher tendency to evaporate than the polymer's primary solvent (DMF). Thus, while both solvents evaporated during the bending instability phase,[43] the lower boiling point solvent is expected to evaporate at a more rapid pace, separating CuI from the solution and allowing the development of crystalline order (vide infra). At the same time, the development of fresh fibers continued. In this regard, the applied voltage plays a key part in controlling the solvent evaporation rate. At higher applied voltages, the solvent evaporates faster, leading to an earlier generation of new fibers.[44] Consequently, the loss of most of the TEA and some of the DMF results in two outcomes: CuI separates from the homogeneous spinning solution, most of which is still within the jet but not in soluble form. Simultaneously the PS solution in the electrospun jet becomes more viscous during the bending and stretching stages and incorporates the separated CuI. This explains why the spinning solutions of higher PS% retained a higher mean proportion of CuI. Conversely, by this model spinning solutions with lower PS% will not be sufficiently viscous to effectively gain more CuI during bending and stretching (see below).

The electrospun fibers were subject to a morphology and elemental analysis using SEM–EDX. Figure 2 shows

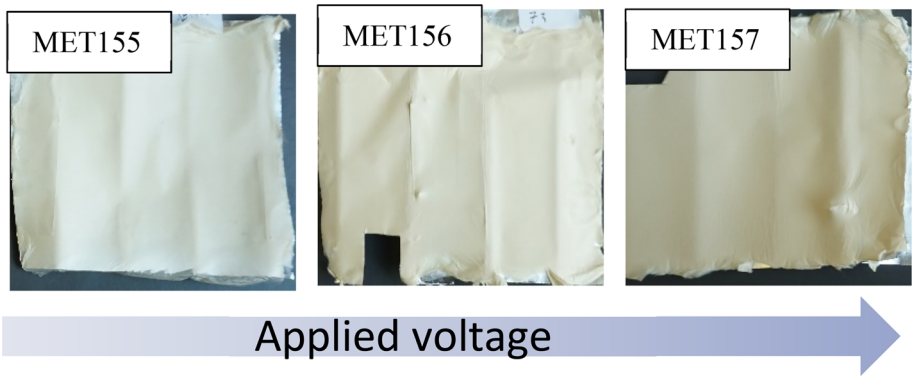

FIGURE 1 Images of electrospun composite fibers spun from the same electrospinning solution of a fixed amount of both PS and CuI but at different spinning voltage. The differences in color are most likely due to oxidation of iodide to iodine rather than small differences in the similar concentrations of the oxidizable CuI. [Color figure can be viewed at wileyonlinelibrary.com]

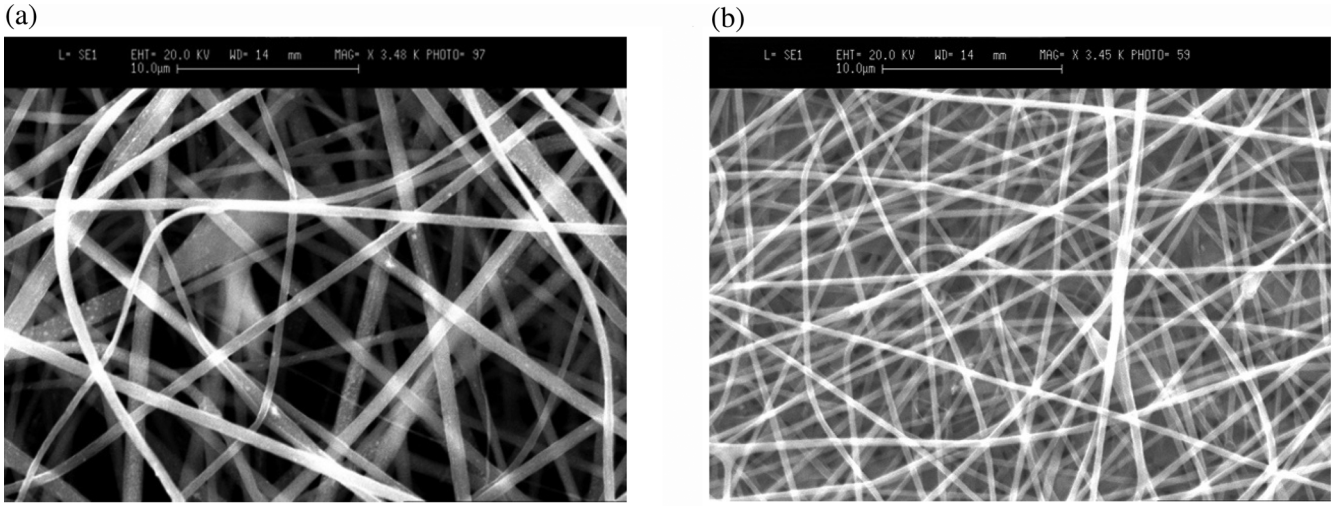

FIGURE 2 SEM images related to the electrospun fibers (a) Sample 157 with a relatively high loading of copper iodide and (b) Sample 161 with an unexpectedly low loading of the cuprous compound (for other micrographs see supporting information).

FIGURE 3 Example of the SEM–EDX analysis; in this case for sample MET156. [Color figure can be viewed at wileyonlinelibrary.com]

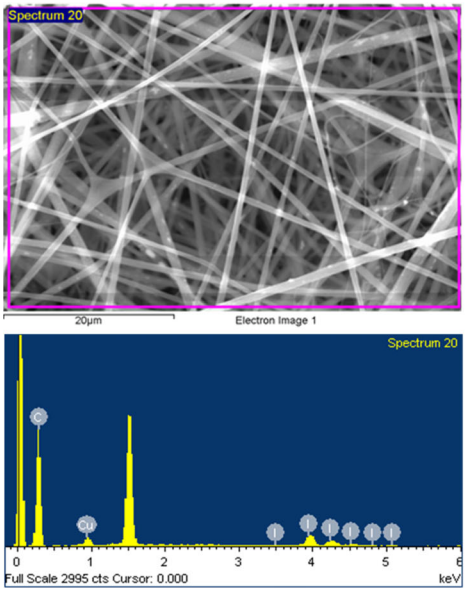

Element	Weight%	Atom%
C K	78.74	96.70
Cu K	7.15	1.66
I L	14.10	1.64
Totals	100.00	

examples of micrographs from the samples (further examples are provided in the supporting information); it was found (with the exception of sample MET 163) that all the conditions listed in Table 2 produced excellent yields of electrospun fibers which were smooth and free of beads. Measurement of the average diameter showed a wide range from 260 to 700 nm depending on polymer concentration and spinning conditions. The EDX experiments confirmed the presence of copper for all samples analyzed; iodine was also detected in most cases, however, for some samples iodine levels were substantially lower than the copper and where the copper concentrations were found to be low often proved difficult to detect (this we attribute to partial oxidation of the iodide ions to volatile iodine, which resulted in the levels dropping below the threshold for detection see supporting information). As the micrograph in Figure 2a shows, there are bright regions suggestive of different material (presumably cuprous iodide). The scale of these regions vary, a few were found to have diameters of several 100 nanometers, but the majority with diameters below 100 nm; mostly these regions appear contained within the fiber. The general pattern from Figure 2a is of a relatively even distribution across the whole fiber. For the most part the surfaces of the fibers are relatively smooth indicating no comparatively large scale structures protruding from the polymer surface.

The diameters of the fibers were measured from data such as that in Figure 2 using ImageJ software (see Materials and Methods above). The proportion of copper is estimated from the EDX data (an example of which is provided in Figure 3 for sample MET156) using the %

Cu data after normalizing to account for the presence of adventitious aluminium or aluminium oxide if required. The data obtained from these fibers are summarized in the tables below; Table 3 shows the effect of varying the polymer concentration with a constant initial copper iodide concentration; Table 4 shows the effect of varying the copper iodide concentration at a constant polymer concentration; in all cases three different voltages were applied.

As inspection of Tables 3 and 4 show, there is a clear correlation between the spinning conditions and the results in terms of copper concentration and fiber diameter. For clarity these data are plotted in Figure 4 and Figure 5. Variation of PS concentrations as shown in Figure 4a showed a clear and mostly consistent trend in terms of nanofibre diameter. Specifically higher concentrations of PS led to larger fiber diameters while increasing the voltage led to a reduction in fiber diameter, in line with expectations based on solution viscosity and the effect of high voltage on the spinning polymer.[45] The effect of copper iodide concentration on fiber diameter was less clear cut, in fact both the largest and smallest fiber diameters were produced at 22.5 kV; presumably here there are competing influences between less substantial changes in the viscosity of the polymer solution and variations in the electrical properties of the mixture.

Figure 5 shows data for the amount of copper present in fibers as calculated by EDX. Unsurprisingly, as shown in Figure 5b increasing the initial copper concentration resulted in higher concentrations of copper in a broadly proportionate way. Within these samples it can be seen that the applied voltage has some effect on the resultant yield of copper within the fibers, and higher voltages produce fibers with higher copper

TABLE 3 Summary of SEM–EDX showing the average weight of Cu and mean diameter of electrospun fibers from three concentrations of PS content, with a fixed CuI content (3%), at three applied voltage levels.

EXP code	PS/% w/v	Applied voltage/ kV	Avg. wt of Cu measured in sample/%	Expected wt of copper/%*	Avg. Dia./nm
MET152	16	17.5	4.45	5.27	687
MET153	16	20	4.89	5.27	630
MET154	16	22.5	5.43	5.27	474
MET158	12.8	17.5	4.53	6.34	452
MET159	12.8	20	5.33	6.34	477
MET160	12.8	22.5	5.56	6.34	391
MET161	10.4	17.5	1.25	7.47	332
MET162	10.4	20	1.89	7.47	267
MET163	10.4	22.5	0.90	7.47	255

*Based on initial amounts of CuI and polystyrene.

TABLE 4 Summary of SEM–EDX results of average weight of Cu and mean diameter of spun fibers of three PS solutions, of variable CuI content, at three applied voltage levels.

Sample	Applied voltage/kV	CuI/%(w/v)	Avg. wt of Cu measured in sample/%	Expected wt of Cu/%*	Avg. Dia. (nm)
MET149	17.5	1	0.76	1.96	510
MET150	20	1	1.88	1.96	653
MET151	22.5	1	3.13	1.96	595
MET152	17.5	3	4.45	5.27	687
MET153	20	3	4.89	5.27	630
MET154	22.5	3	5.43	5.27	474
MET155	17.5	5	5.91	7.94	552
MET156	20	5	7.15	7.94	730
MET157	22.5	5	7.58	7.94	841

*Based on initial amounts of CuI and polystyrene.

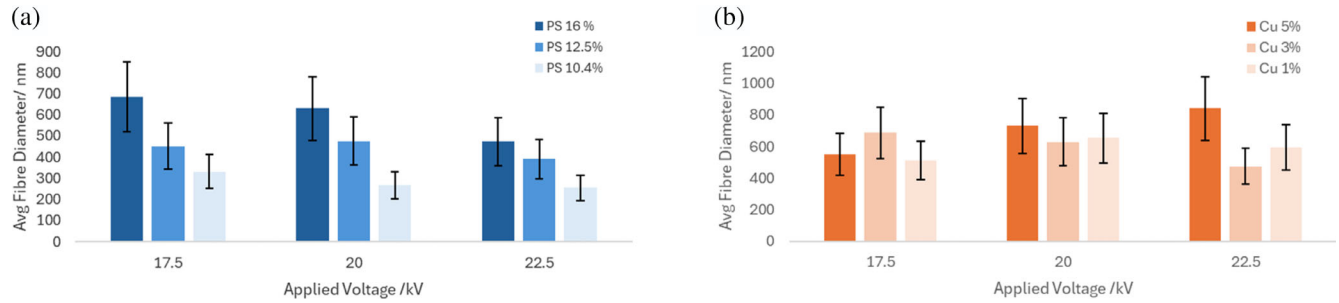

FIGURE 4 The influence of applied voltage on the average diameter with variation of (a) polystyrene concentration and with (b) varying copper concentrations (error bars estimated on the basis of repeated experiments). [Color figure can be viewed at wileyonlinelibrary.com]

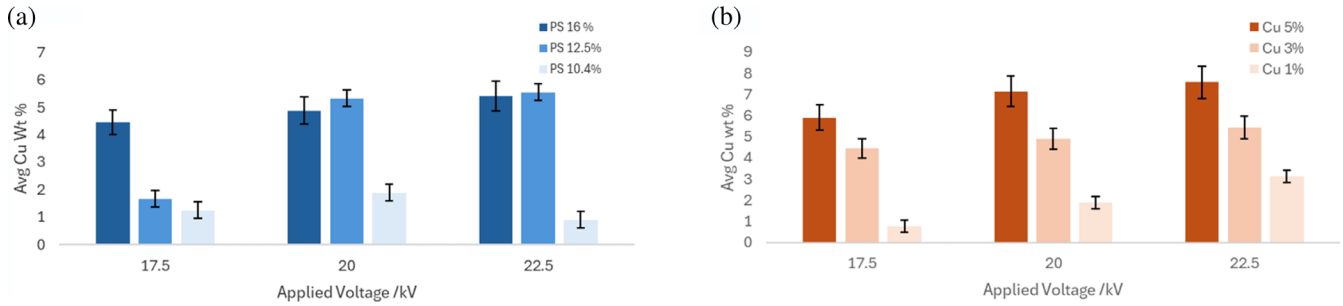

FIGURE 5 The influence of applied voltage on the weight percentage of Cu content in spun fibers with (a) variation of polystyrene concentration and (b) with varying copper concentrations (error bars estimated on the basis of repeated measurements). [Color figure can be viewed at wileyonlinelibrary.com]

concentrations. This relationship between copper concentration and voltage was generally also observed for the experiments in which the concentration of polystyrene was varied as shown in Figure 5a with the exception of PS = 10.4% which produced low concentrations of copper in all cases.

The results above indicate that spinning at higher PS concentrations is a more efficient electrospinning process for the production of nanofibres with higher Cu% content; higher voltages are also helpful in this regard. We suggest that a critical factor in the preparation of such fibers is solution viscosity; thus at the lower polymer concentrations it proved quite challenging to produce fibers, and even successful spinning was accompanied by some spraying. The less viscous solutions, while producing perfectly adequate fibers, were found to contain low amounts of the inorganic component. In addition to this, a relatively high loading of the inorganic species was required; in this regard the presence of TEA was critical. Given this latter solvent has a much lower boiling point than DMF, evaporation of this solvent seems to be a likely factor in the process. This rate of evaporation is likely to be increased as increasing voltage causes the jet to whip and spin and this may account for the trends seen in Figure 5. Thus, the presence of larger amounts of the copper species and the high voltage are likely to increase the speed of the solvent evaporation; the voltage by increasing the forces on the jet and the inorganic material most likely by increasing the conductivity due to the inevitable presence of ionic impurities. Both these factors will increase the speed of the electrospinning jet.[46] In particular, it seems likely that where copper iodide is precipitated early on in the process it remains in the viscous substrate, crystal growth may continue albeit at a decreasing rate as the viscosity increases. For the lower concentration PS solutions this viscosity is likely to be lower, this suggests there is potential for larger crystallites developing; additionally, the fibers produced tended to have a smaller diameter and this size mismatch reduces the possibility of encapsulation of cuprous iodide within the polymer. Alternatively there may be some phase separation of polymer from the solutions[47] and the non-polymer component may spray due to the whipping motion of the fiber. This would result in the solution being deposited (and subsequently evaporating) on the electrode. EDX analysis further confirms a broadly proportional relationship between the amount of CuI in the spinning solutions and the mean Cu wt% content of the produced nanofibres, particularly for the most concentrated PS solution as shown Figure 5b.

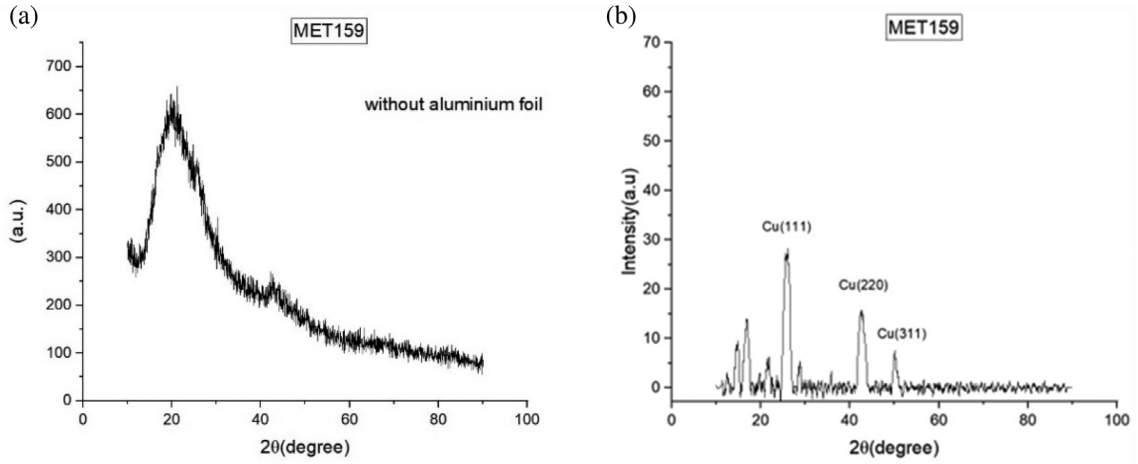

FIGURE 6 (a) Scattering pattern obtained from composite fiber sample 159, (b) result of subtraction of the broad scattering pattern due to polystyrene.

While these broadly positive results were encouraging there were some issues with nature of the fibers presenting with lower copper concentration, in particular, in many cases EDX showed iodine content much smaller than that of the copper in terms of atom % (see supporting information Table S1). For example for MET 149 the Cu:I atom% was close to 2:1, for MET 153 the ratio was 1:0.7; in contrast MET 156 and MET 157 showed values close to the expected 1:1. In addition in many cases powder X-ray studies showed unexpected peaks and an absence of diagnostic peaks for cuprous iodide. This is discussed further below.

For the fiber samples with higher concentrations of copper the XRD analysis confirmed the presence of CuI, although the analysis was complicated by the presence of additional features. Thus, in all cases any sharp Bragg peaks arising from inorganic crystalline material were superimposed on broad peaks arising from PS centred at about 20° and 45°. In many examples it proved difficult to separate the sample from the aluminium foil and consequently additional peaks were seen due to this and consequent aluminium oxides or hydroxide. A further complication was that in some cases peaks appeared which suggest the oxidation of copper and potentially disproportionation. It was also found peaks from CuI were often broad, and in many cases only readily seen by baseline subtraction. For example, Figure 6a shows what superficially appears as a typical X-ray scattering pattern from an amorphous PS sample; however closer inspection reveals Bragg peaks superimposed on the broad peak at around $2\theta = 25°$, 42°, and 50°. We have adopted a smoothing and subtraction procedure which results in the pattern observed in Figure 6b, the three peaks can be clearly assigned to cuprous iodide and their positions are diagnostic of the zinc blend structure typical for this crystal at room temperature with peak positions at $2\theta = 25.7°$ (111), 42.4° (220), and 50.1° (311).[48] Of the additional peaks present, a peak at 29.3° could also relate to CuI (220) other peaks are mostly present in all samples coated on foil and relate to Aluminium, or aluminium oxides (see supporting information) with an exception of a peak ca. 43° which possibly relates to the presence of copper as discussed below.

In many cases the presence of additional peaks made assignment of the diffraction pattern difficult even following removal of the PS signal. Figure 7 shows the scattering pattern obtained from MET 157, that is, the sample with the largest copper concentration in the polymer sample. As can be seen there are three peaks with positions appropriate for CuI, however only the peak around 25.7° is clearly distinguished. The peak at 42.4° is overlapping with a more intense one at 41.9°; together with the peak at 43.3° (very weak in this case) which is suggestive of copper metal, FCC (111).[49] The peak at 50.1° is relatively low intensity in line with the literature diffraction pattern for CuI (and would potentially overlap with diffraction from copper metal if this was present in significant amounts).

In view of the overlap and intensity issues with high angle peaks our further examination of the morphology focused on the peak at $2\theta = 25°–26°$. In particular, substantial variations in the line width of this peak were noted. This can be seen in the partial diffraction patterns shown in Figure 8. The line width can be used to determine the crystallite size via the well-known Scherrer formula[50]; this relates the full width at half maximum intensity to the size of crystallites, we calculated values for a number of samples. For sample MET 157, which were found to be the fibers with the highest loading of CuI, an intense peak is observed at $2\theta = 25.7°$ with a line

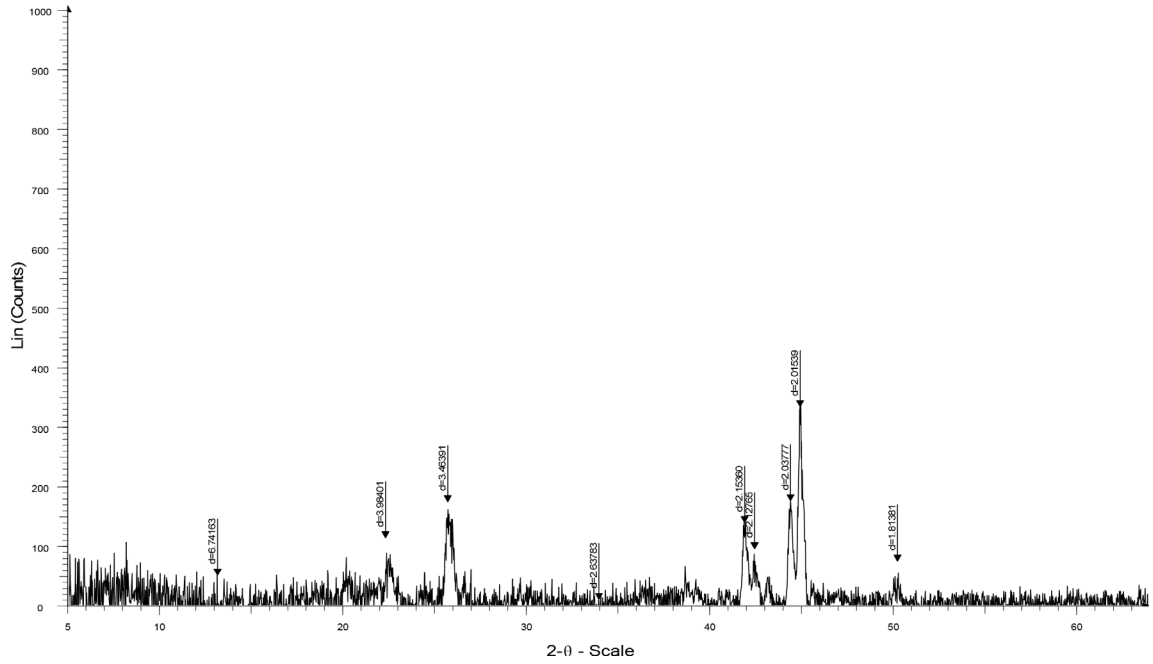

FIGURE 7 X-ray diffraction pattern obtained for electrospun fiber sample MET 157 following removal of the amorphous signal due to polystyrene.

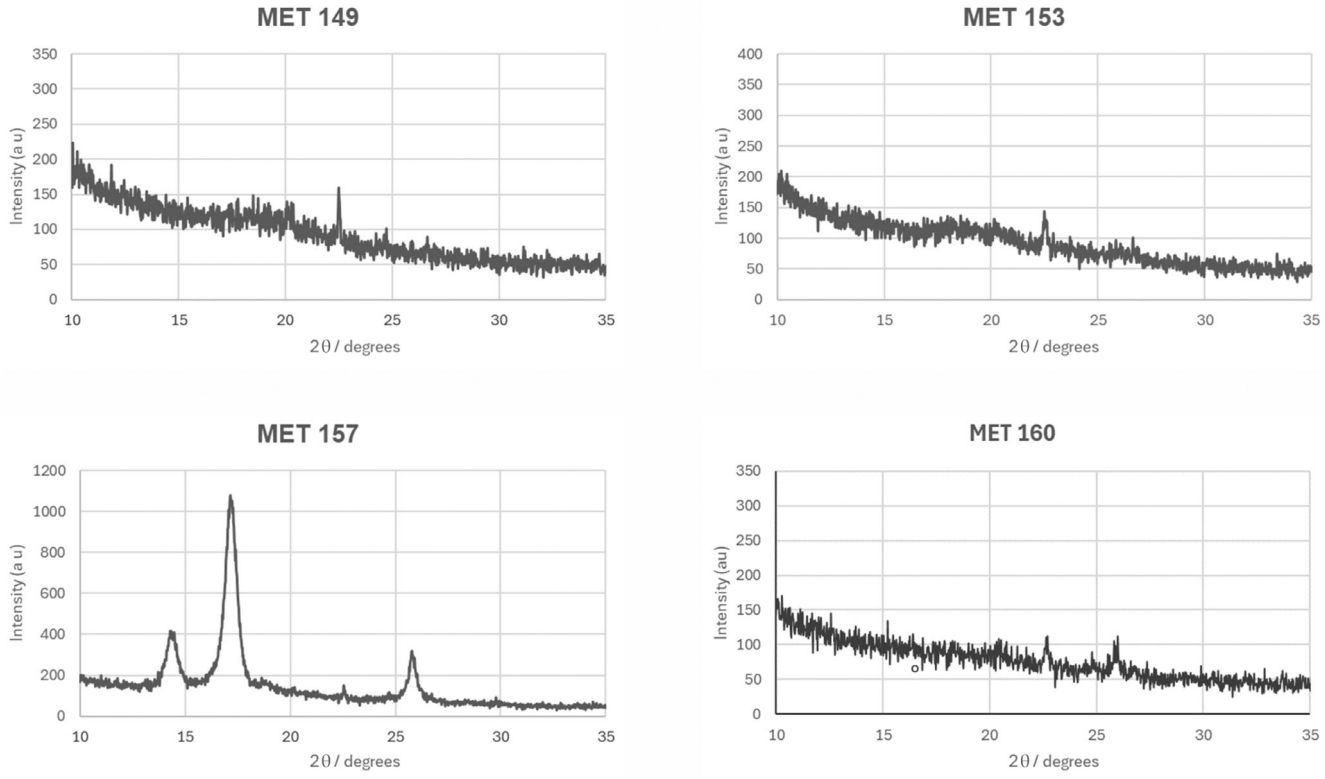

FIGURE 8 Different scattering from the CuI .111 plane for polystyrene copper iodide composite fibers.

width of 0.35°, from which a crystallite size of 24 nm is calculated. The corresponding peak with sample MET 160 (in fact at $2\theta = 25.8°$) showed a width of 0.6°, indicating a crystallite size of 14 nm. For sample MET153, a much broader less well defined line (centred at $2\theta = 26.2°$) gave by the same analysis a line width of 1.5° suggesting crystallites sizes of 6 nm. That being said, the shift in the peak position and the rather broad line shape

means that the assignment of this peak to γ CuI is at best uncertain. Given this type of broadened peak was apparent for a number of samples within the constraints of the signal to noise, a more likely scenario is the formation of another copper-based species, particularly in view of the low iodine concentrations present in many samples (vide supra). For Sample MET 149 no scattering from CuI was apparent either due to the low CuI concentration, line broadening, or both.

In order to further understand the copper concentration details from the SEM/EDX measurements, and particularly the low amounts of copper found at some spinning conditions, we undertook measurements of the bulk copper concentration from a selection of samples using Inductively Coupled Plasma Mass Spectrometry. The results obtained are listed in Table 5 together with the data from the EDX samples and the initial copper concentrations. Where sufficient sample was available, a duplicate reading from a different section of the fiber mat was taken. As expected, on the basis of the differences between initial copper concentrations and EDX values, some of the samples were quite inhomogeneous, for example the data for two samples of MET 153 showed significant differences (ca. 40%) and the values were rather lower than found in the fibers by EDX. This clearly reflects an uneven distribution of copper in these samples. Repeat values for MET 158 MET 159 and MET 160 however, were rather closer with differences around 10%.

TABLE 5 Summary of SEM–EDX results of average weight of Cu and Copper concentration of bulk samples from ICP-MS.

Sample	Expected wt of Cu /%*	EDX Avg. wt of Cu in sample/%	ICP-MS Avg. wt of Cu in sample/%†
MET149	1.96	0.76	1.01
MET153	5.27	4.89	2.48 (3.53,1.43)
MET154	5.27	5.43	5.10
MET155	7.94	5.91	7.41 (8.20, 6.61)
MET156	7.94	7.15	7.67
MET157	7.94	7.58	7.16
MET158	6.34	4.53	7.07 (6.77, 7.37)
MET159	6.34	5.33	6.93 (6.62, 7.23)
MET160	6.34	5.56	7.21 (6.82, 7.60)
MET161	7.47	1.25	5.58
MET162	7.47	1.89	5.27
MET163	7.47	0.9	5.61

*Based on initial solution concentrations.
†Results of duplicate readings in brackets.

For the most part, within the limits of experimental error the data in Table 5 is consistent with most of the copper from the initial solution being incorporated in the sample if not in the fiber. This assumes there is no substantial loss of iodine which would substantially increase the expected proportion of copper (e.g., for MET 158 if the copper was present as copper oxide rather than copper iodide we might expect 7.12% rather than 6.34%). Thus, for the majority of samples the bulk copper concentrations were rather higher than found in the fibers and we believe this reflects the contribution to the copper concentration from copper lost to the fiber via spraying. This is particularly apparent for Samples MET 161–163; here copper concentrations are very much higher than was observed in the fibers, but significantly lower than the initial concentrations. These three samples were produced at the lowest PS concentrations, were the most challenging to spin, and had by far the largest discrepancy between the initial CuI concentration, and that detected in the fibers. The production of these fibers was in many cases accompanied by spraying and it is presumably this that accounts for the anomalous values. A fine spray would be more likely to penetrate the samples, end up close to the collector surface and thus remain largely separate from the fibers, and also spread over a wider area; thus, in this case concentrations remain lower than the amount inputted. As a consequence, for the examples with low PS concentration, the copper is not found in great amounts in the fiber, but rather is present close to the collector, and spread over a wider area; for other samples spraying is likely to occur but the copper is largely confined to the fiber mat. In contrast, samples MET 156 and MET 157 exhibited concentrations close to the initial values and also close to the values determined by EDX indicating the copper is largely contained within or attached to the fibers, thereby producing a fairly homogeneous system.

On the basis of the SEM, EDX, and XRD studies we have developed a mechanism for this electrospinning process. Successful development of composite fibers appears to occur when there is sufficient time for the copper iodide to develop crystallites with sizes above about 20 nm. This in turn seems to require precipitation of the inorganic species before polymer solidification. This is the case if the more volatile TEA is removed early in the process, as there is time for crystallization and agglomeration of the copper and iodine ions into a regular structure. Where this does not happen, in some cases it may be that copper iodide may be retained in unevaporated solvent and on the basis of the ICP-MS studies probably lost as spray. The appearance of additional Bragg peaks in the XRD experiment and unexpected low levels of

iodine in the EDX samples suggest that during the fiber formation process, iodide may be lost, most likely via oxidation. In such circumstances the excess Cu^{+} ions unable to coordinate with I^{-} will become unstable and disproportionate to form an unidentified copper (II) species (presumably oxygen coordinated) and copper metal which accounts for the peak at $2\theta = 43.3°$ as shown in Equation (1).

$$2Cu^{+} \longrightarrow Cu^{0} + Cu^{++} \quad (1)$$

4 | CONCLUSION

In this work we set out to find route to and thus prepare composite nanofibres of a polymer and copper(I) iodide. We have successfully produced composite nanofibres of CuI-PS using electrostatic spinning. A combination of dual solvents was utilized to achieve a homogeneous solution of polymer and CuI. The process involved a volatile solvent and carrier for the inorganic species and a less volatile solvent for the polymer. Careful control of solution preparation (dissolving without heat or excessive agitation) was found to be important in the generation of smooth fibers at all concentrations. It was found that both PS concentration and the applied voltage control the fiber morphology and the copper iodide percentage in the electrospun fibers. The potential for reaction of the active component during the spinning process (likely facilitated by the high surface areas) is an important consideration in the preparation of such samples, necessitating a detailed analysis of the fibers produced. It was determined that polymer solutions of higher PS concentration and a higher applied voltage were required to retain a higher content of CuI. Without the careful control of all these factors production of these composites is unlikely to be successful.

AUTHOR CONTRIBUTIONS

Muaathe A. Ibraheem: Conceptualization (lead); investigation (lead); methodology (lead); writing – original draft (lead). **Fred J. Davis:** Supervision (supporting); writing – review and editing (supporting). **Saeed D. Mohan:** Writing – review and editing (supporting). **John E. McKendrick:** Supervision (supporting); writing – review and editing (supporting).

ACKNOWLEDGMENTS

The authors would like to acknowledge the support given by Iraqi cultural attaché and Prof. Dr. Tahseen H. Mubarak for his personal assistance and support. We would also like to thank Amanpreet Kaur for her help with scanning electron microscopy Nick Spencer with his help in obtaining XRD data and Andy Dodson for help with the ICP-MS data. We thank Prof. Ann Chippindale for helpful discussions. This research was supported by the University of Reading Chemical Analysis Facility (CAF). We also thank the University of Tehran for help in obtaining some additional SEM and XRD data

CONFLICT OF INTEREST STATEMENT

The authors declare no conflict of interest influencing the representation or interpretation of re-ported research results.

DATA AVAILABILITY STATEMENT

The data that support the findings of this study are available from the corresponding author upon reasonable request.

ORCID

Muaathe A. Ibraheem https://orcid.org/0000-0003-0128-7130
Fred J. Davis https://orcid.org/0000-0003-0462-872X
Saeed D. Mohan https://orcid.org/0000-0001-5388-088X
John E. McKendrick https://orcid.org/0000-0003-2275-0569

REFERENCES

[1] S. J. Sowerby, N. G. Holm, G. B. Petersen, *Biosystems* **2001**, *61*, 69.
[2] S. F. Hansen, A. Maynard, A. Baun, J. A. Tickner, D. M. Bowman, *Nat. Nanotechnol.* **2008**, *3*, 444.
[3] C. T. Lim, *Prog. Polym. Sci.* **2017**, *70*, 1.
[4] M. Mirjalili, S. Zohoori, *J. Nanostructure Chem.* **2016**, *6*, 207.
[5] M. Badmus, J. Liu, N. Wang, N. Radacsi, Y. Zhao, *Nano Mater. Sci.* **2021**, *3*, 213.
[6] R. Sahay, P. S. Kumar, R. Sridhar, J. Sundaramurthy, J. Venugopal, S. G. Mhaisalkar, S. Ramakrishna, *J. Mater. Chem.* **2012**, *22*, 12953.
[7] N. N. Bui, M. L. Lind, E. M. V. Hoek, J. R. McCutcheon, *J. Membr. Sci.* **2011**, *385*, 10.
[8] R. P. Dumitriu, G. R. Mitchell, F. J. Davis, C. Vasile, *Procedia Manuf.* **2017**, *12*, 59.
[9] H. Mu, C. Li, J. Bai, W. Sun, *J. Mol. Struct.* **2018**, *1165*, 90.
[10] A. J. Meinel, O. Germershaus, T. Luhmann, H. P. Merkle, L. Meinel, *Eur. J. Pharm. Biopharm.* **2012**, *81*, 1.
[11] H. C. Yeom, D. J. Moon, K. Y. Lee, S. W. Kim, *J. Nanosci. Nanotechnol.* **2015**, *15*, 5167.
[12] A. K. Figen, B. C. Filiz, *J. Colloid Interface Sci.* **2019**, *533*, 82.
[13] B. Wang, L. Luo, Y. Ding, D. Zhao, Q. Zhang, *Colloids Surf. B Biointerfaces* **2012**, *97*, 51.
[14] X. Liang, D. Zhao, L. Wang, Q. Huang, C. Deng, L. Wang, L. Hu, S. Liang, H. Deng, H. Xiang, *Energy Mater.* **2023**, *3*, 300006.
[15] Z. E. Zadeh, A. Solouk, M. Shafieian, M. H. Nazarpak, *Mater. Sci. Eng. C* **2021**, *118*, 111403.
[16] M. Nazhipkyzy, S. D. Mohan, F. J. Davis, G. R. Mitchel, *J. Phys. Conf. Ser.* **2015**, *246*, 012007.

[17] S. Chen, Y. Guo, D. Yuan, C. He, J. Bao, S. Ai, F. Li, W. Zhao, Y. Xu, C. Zhao, *Compos. Sci. Technol.* **2021**, *214*, 108993.
[18] M. Aravind, M. Amalanathan, S. Aslam, A. E. Noor, D. Jini, S. Majeed, P. Velusamy, A. A. Alothman, R. A. Alshgari, M. S. S. Mushab, M. Sillanpaa, *Chemosphere* **2023**, *321*, 138077.
[19] B. Sahoo, P. K. Panda, S. Ramakrishna, *Open Ceram.* **2022**, *11*, 100291.
[20] M. Bognitzki, M. Becker, M. Graeser, W. Massa, J. H. Wendorff, A. Schaper, D. Weber, A. Beyer, A. Gölzhäuser, A. Greiner, *Adv. Mater.* **2006**, *18*, 2384.
[21] Q. Sun, X. Shi, X. Wang, Y. Zhai, L. Gao, Z. Li, Y. Hao, Y. Wu, *Org. Electron.* **2019**, *75*, 105428.
[22] J. Quirós, J. P. Borges, K. Boltes, I. Rodea-Palomares, R. Rosal, *J. Hazard. Mater.* **2015**, *299*, 298.
[23] L. Muthukrishnan, *Colloid Polym. Sci.* **2022**, *300*, 875.
[24] N. Joudeh, D. Linke, *J Nanobiotechnol* **2022**, *20*, 262.
[25] H. A. Atwater, *Sci. Am.* **2007**, *296*, 56.
[26] M. Muldarisnur, I. Perdana, E. Elvaswer, D. Puryanti, *Emerging Science Journal* **2023**, *7*, 1083.
[27] S. D. Prasetyo, E. P. Budiana, A. R. Prabowo, Z. Arifin, *Civil Engineering Journal* **2023**, *9*, 2989.
[28] H. Hori, T. Teranishi, Y. Nakae, Y. Seino, M. Miyake, S. Yamada, *Phys. Lett. A* **1999**, *263*, 406.
[29] M.-H. Lv, C.-M. Li, W.-F. Sun, *Nano* **2022**, *12*, 382.
[30] S. P. Łepkowski, W. Bardyszewski, *Sci. Rep.* **2018**, *8*, 2.
[31] M. Huangfu, Y. Shen, G. Zhu, K. Xu, M. Cao, F. Gu, L. Wang, *Applied Surface Science Part B* **2015**, *357*, 2234.
[32] R.-Y. Zhao, R.-D. Xu, G.-N. Liu, Y. Sun, C. Li, *Inorg. Chem. Commun.* **2019**, *105*, 135.
[33] Q.-W. Guan, D. Zhang, Z.-Z. Xue, X.-Y. Wan, Z.-N. Gao, X.-F. Zhao, C.-P. Wan, J. Pan, G.-M. Wang, *Inorg. Chem. Commun.* **2018**, *95*, 144.
[34] S. Hull, D. A. Keen, W. Hayes, N. J. G. Gardner, *J. Phys. Condens. Matter* **1998**, *10*, 10941.
[35] J. Huang, D. Lu, T. Mandal, *Synth. Commun.* **2021**, *51*, 1923.
[36] Y. Takeda, D. Jamsransuren, T. Nagao, Y. Fukui, S. Matsuda, H. Ogawa, *Appl. Environ. Microbiol.* **2021**, *87*, e01824.
[37] A. Pramanik, D. Laha, D. Bhattacharya, P. Pramanik, P. Karmakar, *Colloids Surf. B. Biointerfaces* **2012**, *96*, 50.
[38] H. B. Kim, W. J. Lee, S. C. Choi, K. B. Lee, M. H. Lee, *Aerosol Sci. Technol.* **2020**, *55*, 154.
[39] M. Sushmita, Patel, D. Thakur, A. K. Verma, *Org. Biomol. Chem.* **2023**, *21*, 2301.
[40] K. A. Narh, P. J. Barham, A. Keller, *Macromolecules* **1982**, *15*, 464.
[41] J. Zhong, S. D. Mohan, A. Bell, A. Terry, G. R. Mitchell, F. J. Davis, *Int. J. Biol. Macromol.* **2018**, *113*, 764.
[42] G. B. Kauffman, L. Y. Fang, N. Viswanathan, G. Townsend, in *Inorganic Syntheses* (Ed: S. L. Holt), Wiley Online Library, Hoboken, New Jersey **1984**.
[43] A. L. Yarin, S. Koombhongse, D. H. Reneker, *J. Appl. Phys.* **2001**, *89*, 3018.
[44] S. Tripatanasuwan, Z. Zhong, D. H. Reneker, *Polymer* **2007**, *48*, 5742.
[45] F. J. Davis, S. D. Mohan, M. A. Ibraheem, in *Electrospinning: Principles, Practice and Possibilities* (Ed: G. R. Mitchell), The Royal Society of Chemistry, Cambridge **2015**, p. 1 Chapter. 1.
[46] C. Wang, C.-H. Hsu, J.-H. Lin, *Macromolecules* **2006**, *39*, 7662.
[47] J. Avossa, G. Herwig, C. Toncelli, F. Itel, R. M. Rossi, *Green Chem.* **2022**, *24*, 2347.
[48] Y. Shan, G. Li, G. Tian, J. Han, C. Wang, S. Liu, H. Du, Y. Yang, *J. Alloys Compd.* **2009**, *477*, 403.
[49] R. Betancourt-Galindo, P. Y. Reyes-Rodriguez, B. A. Puente-Urbina, C. A. Avila-Orta, O. S. Rodríguez-Fernández, G. Cadenas-Pliego, R. H. Lira-Saldivar, L. A. García-Cerda, *J. Nanomater.* **2014**, *2014*, 980545.
[50] D. M. Smilgies, *J. Appl. Crystallogr.* **2009**, *42*, 1030.

SUPPORTING INFORMATION

Additional supporting information can be found online in the Supporting Information section at the end of this article.

How to cite this article: M. A. Ibraheem, F. J. Davis, S. D. Mohan, J. E. McKendrick, *J. Appl. Polym. Sci.* **2024**, e56322. https://doi.org/10.1002/app.56322